COMMUNICATIONS IN INFORMATION AND SYSTEMS
Vol. 3, No. 3, pp. 191-202, March 2004

© 2004 International Press
004

VOLUMETRIC HARMONIC MAP*

YALIN WANG†, XIANFENG GU‡, AND SHING-TUNG YAU§

Abstract. We develop two different techniques to study volume mapping problem in Computer Graphics and Medical Imaging fields. The first one is to find a harmonic map from a 3 manifold to a 3D solid sphere and the second is a sphere carving algorithm which calculates the simplicial decomposition of volume adapted to surfaces. We derive the 3D harmonic energy equation and it can be easily extended to higher dimensions. We use a textrehedral mesh to represent the volume data. We demonstrate our method on various solid 3D models. We suggest that 3D harmonic mapping of volume can provide a canonical coordinate system for feature identification and registration for computer animation and medical imaging.

1. Introduction. With the rapid development of imaging technology, there has been an explosive growth of three-dimensional (3D) image data collected from all kinds of physical sensors. The technique to process and analyze these image data becomes important. In this paper, we develop two different techniques to study volume mapping problem in Computer Graphics and Medical Imaging fields. One of our techniques is to compute a harmonic map from a 3 manifold to a 3D solid sphere. To the best of knowledge, it is the first work to practically compute 3D harmonic map between 3D volumes. The other technique is to calculate the simplicial decomposition of volume adapted to surfaces. Compared with existed Finite Element Method (FEM) mesh generation, our new technique emphasizes geometry and topology sanity maintenance.

The functional space on a manifold is determined by the manifold geometric characteristics. The harmonic spectrum can reflect many global geometric information of the manifold. Some applications on computer graphics and medical imaging fields, such as volume registration, shape analysis, etc. can be carried out by examining the behavior of special differential operators on it. In the literature, some researchers used harmonic map for surface matching [1] and the construction of conformal map for genus zero surfaces [2, 3]. For 3D brain volume transformation research, Gee [4] studied brain volume matching with a generalized elastic matching method within a probabilistic framework. The approach can resolve issues that are less naturally addressed in a continuum mechanical setting. Ferrant et al. [5] presented an algorithm for non-rigid registration of 3D MR intraoperative image sequences showing brain shift. The 3D anatomic deformation field, in which surfaces are embedded, is then inferred from the displacements at the boundary surfaces using a biomechanical finite element model for the constituent objects.

In 2D case, a harmonic map between two convex planar regions is diffeomorphic if and only if the restriction on the boundary is diffeomorphic. 3D harmonic map is much more

---

complicated. In this paper, we construct a harmonic map in $\mathbb{R}^3$ with a heat flow method. First we conformally map the boundary of the 3D volume to a sphere, then minimizes the volumetric harmonic energy while keeping the surface fixed. We also show how the interior of the volume changes when we apply a Möbius transformation on the surfaces. To the best of our knowledge, this is the first work on volumetric harmonic map. This work is also quite general and can easily be generalized to higher-dimensional cases.

In the last decade, the techniques of 3D cameras, Computed Tomography (CT) and Magnetic Resonance Imaging (MRI) developed rapidly. Computer visualization and engineering calculation require certain kinds of mesh extracted from these scanned volume data. Although there are many researches on the mesh generation [6, 7], the existed methods usually do not pay enough attention to geometry and topology checking. Thus the resulting mesh structure cannot be directly used for geometry analysis computation. We developed a sphere carving algorithm to calculate the simplicial decomposition of volume adapted to surfaces. From the volume data, our algorithm can build tetrahedral mesh with desired geometry and topology characteristics.

The remainder of the paper is organized as follows. In Section 2, we give the definitions of harmonic energy and a detailed description of our algorithm. Section 3 reports our sphere carving algorithm. Section 4 shows our experiments on various 3D solid models. We conclude the paper with the discussion of future research directions in Section 5.

2. Volumetric Harmonic Mapping Algorithm.

2.1. Definitions. Suppose K is a simplicial complex, and $f : |K| \to \mathbb{R}^3$, which embeds $|K|$ in R^3; then (K, f) is called a mesh. Given a genus zero tetrahedral mesh M, our goal is to compute its harmonic map to a sphere in $\mathbb{R}^3$.

DEFINITION 1. *All piecewise linear functions defined on K form a linear space, denoted by $C^{PL}(K)$*

DEFINITION 2. *Suppose a set of string constants $k(u,v)$ are assigned, then the inner product on C^{PL} is defined as the quadratic form:*

$$(1) \qquad < f, g > = \frac{1}{2} \sum_{\{u,v\} \in K} k(u,v)(f(u) - f(v))(g(u) - g(v)).$$

The energy is defined as the norm on C^{PL}

DEFINITION 3. *Suppose $f \in C^{PL}$, the string energy is defined as:*

$$(2) \qquad E(f) = < f, f > = \sum_{\{u,v\} \in K} k(u,v)||f(u) - f(v)||^2.$$

By changing the string constants $k(u,v)$ in the energy formula, we can define different string energies.

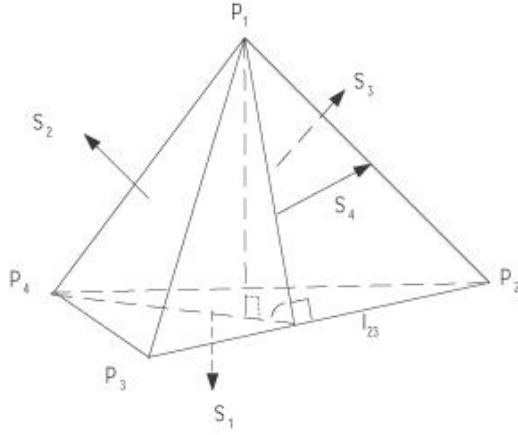Below is our derivation of harmonic energy in 3 dimensional space.

FIG. 1. *Illustrates a tetrahedron.*

As shown in Figure 1, we define

$$\vec{s}_i = Area(Face\ i)\vec{n}_i, i = 1,2,3,4,$$

where $\vec{n}_i$ is the normal on Face i. Due to $(\vec{s}_i) = -\sum_{j\neq i} <\vec{s}_j, \vec{n}_i>$, and $\vec{n}_i, i = 1,2,3,4$ can uniquely determine a frame in the space, we have

$$\sum_{i=1}^{4} \vec{s}_i = 0$$

and

$$<\vec{s}_i, \vec{s}_i> = -\sum_{i\neq j} <\vec{s}_i, \vec{s}_j>, i = 1,2,3,4.$$

For a random point $\vec{r}$ inside the tetrahedron, its barycentric coordinate is

(3)
$$\vec{r} = \sum_{i=1}^{4} (\lambda_i \vec{p}_i),$$
$$\lambda_i = \frac{1}{3} \frac{<\vec{r}, \vec{s}_i>}{V},$$

where V is the volume of tetrahedron. For a function defined on the tetrahedron,

$$f(\vec{r}) = \sum_{i=1}^{4} \lambda_i f(\vec{p}_i) = \sum_{i=1}^{4} \frac{1}{3} \frac{<\vec{r}, \vec{s}_i>}{V}.$$

Thus we have $\nabla f = \frac{1}{3V} \sum_{i=1}^{4} \vec{s}_i f_i$. Let $I = \{1,2,3,4\}$, the harmonic energy for the tetrahedron

can be computed as

$$E(f) = \frac{V}{2} < \nabla f, \nabla f > = \frac{1}{18V} < \sum_{i=1}^{4} \vec{s}_i f_i, \sum_{i=1}^{4} \vec{s}_i f_i >$$

$$= \frac{1}{18V} (\sum_{i=1}^{4} < \vec{s}_i, \vec{s}_i > f_i^2 + 2 \sum_{i \neq j} < \vec{s}_i, \vec{s}_j > f_i f_j)$$

(4)

$$= -\sum_{i \neq j} \frac{< \vec{s}_i, \vec{s}_j >}{18V} (f_i - f_j)^2$$

$$= \sum_{\substack{i \neq j, p \neq q \\ \{p,q\}=I \setminus \{i,j\}}} l_{pq} \frac{\cot(\theta_{pq})}{12} (f_i - f_j)^2.$$

The last equation in Equation 4 holds due to

$$\frac{< \vec{s}_i, \vec{s}_j >}{V} = -\frac{|\vec{s}_i| \frac{1}{2} l_{pq} h_q \cos(\theta_{pq})}{\frac{1}{3} |\vec{s}_i| h_q \sin(\theta_{pq})} = -\frac{3}{2} l_{pq} \cot(\theta_{pq}),$$

where l_{pq} and h_q are the edge length and height length in triangle q, as shown in Figure 1.
The proof is general and it can be easily generalized to higher dimensional cases.

DEFINITION 4. *Suppose for edge $\{u,v\}$, it is shared by n tetrahedra thus it is against to n dihedral angles, θ_i, $i = 1, \dots, n$. Define the parameters*

(5)
$$k_{u,v} = \frac{1}{12} \sum_{i=1}^{n} l_i \cot(\theta_i)$$

where l_i is the length of edge to which edge $\{u,v\}$ is against in the domain manifold M. The string energy obtained is called the harmonic energy.

DEFINITION 5. *The piecewise Laplacian is the linear operator $\Delta_{PL} : C^{PL} \to C^{PL}$ on the space of piecewise linear functions on K, defined by the formula*

(6)
$$\Delta_{PL}(f) = \sum_{\{u,v\} \in K} k(u,v)(f(v) - f(u)).$$

If f minimizes the string energy, then f satisfies the condition $\Delta_{PL}(f) = 0$. Suppose M_1, M_2 are two meshes and the map $\vec{f} : M_1 \to M_2$ is a map from M_1 to R^3.

DEFINITION 6. *For a map $\vec{f} : M_1 \to R^3$, $\vec{f} = (f_0, f_1, f_2)$, we define the energy as the norm of $\vec{f}$:*

(7)
$$E(\vec{f}) = ||\vec{f}||^2 = \sum_{i=0}^{3} ||f_i||^2.$$

The Laplacian is defined in a similar way.

DEFINITION 7. *For a map $\vec{f} : M_1 \to R^3$, the piecewise Laplacian of $\vec{f}$ is*

(8)
$$\Delta_{PL}\vec{f} = (\Delta_{PL}f_0, \Delta_{PL}f_1, \Delta_{PL}f_2).$$

A map $\vec{f} : M_1 \rightarrow M_2$ is harmonic, if and only if it only has a normal component, and the tangential component is zero.

$$(9) \qquad \Delta_{PL}(\vec{f}) = (\Delta_{PL}\vec{f})^{\perp}.$$

2.2. Steepest Descent Method. Suppose we would like to compute a mapping $\vec{f} : M_1 \rightarrow M_2$ such that $\vec{f}$ minimizes a string energy $E(\vec{f})$. This can be solved easily by the steepest descent algorithm:

$$(10) \qquad \frac{d\vec{f}(t)}{dt} = -\Delta\vec{f}(t)$$

$\vec{f}(M_1)$ is constrained to be on M_2, so $-\Delta\vec{f}$ is a section of M_2's tangent bundle.

Based on the above definitions and algorithm, our volumetric harmonic brain mapping algorithm is given below.

ALGORITHM 1. *Volumetric Harmonic Mapping*

Input (mesh M, step length δt, energy difference threshold δE),

output($\vec{h} : M \rightarrow D^3$), where $\vec{h}$ is a harmonic map.

1. *Compute the surface structure, ∂M, of the mesh M. Compute its conformal mapping to the surface of a sphere, $\vec{g} : \partial M \rightarrow S^2$ [2, 3];*

2. *For each boundary vertex, $v, v \in \partial M$, let $\vec{h}(v) = \vec{g}(v)$; for each interior vertex , $v, v \in M \backslash \partial M$, let $\vec{h}(v) = (0,0,0)$, compute the harmonic energy E_0;*

3. *For each interior vertex, $v \in M \backslash \partial M$, compute its derivative $D\vec{h}$;*

4. *Update $\vec{h}(v)$ by $\delta\vec{h}(v) = -D\vec{h}(t)\delta t$;*

5. *Compute the harmonic energy E;*

6. *If $E - E_0 < \delta E$, return $\vec{h}$. Otherwise, assign E to E_0 and repeat steps 3 through 6.*

3. Sphere Carving Algorithm. Methods to tetrahedralize volume data are well studied for FEM research. However, the methods to tetrahedralize volume with complicated geometric structure such as the brain are somewhat rare in the literature, although they are used occasionally for surgical simulation, or mapping intraoperative brain change. In our current experiments, we apply a sphere carving algorithm to volume data tetrahedralization problem. At the beginning, the algorithm constructs a large sphere that contains all the volume data. For non-genus case, we cut open the sphere to make it have desired genus number. Then the algorithm keeps removing the outside tetrahedra while maintaining the surface genus number. The input image to this algorithm is binary 3D volumetric image. Figure 2(a) shows a few sections from a binary brain volume. Our goal is to build a tetrahedral volume while maintaining a surface with desired genus number. In the case of brain volume construction, we take a sequence of brain MRI images. First it builds a large sphere tetrahedral mesh which totally encloses the brain 3D volume. Then it keeps removing the tetrahedra outside of the brain volume while maintaining a genus zero surface. It outputs a brain tetrahedral mesh with a genus zero boundary.
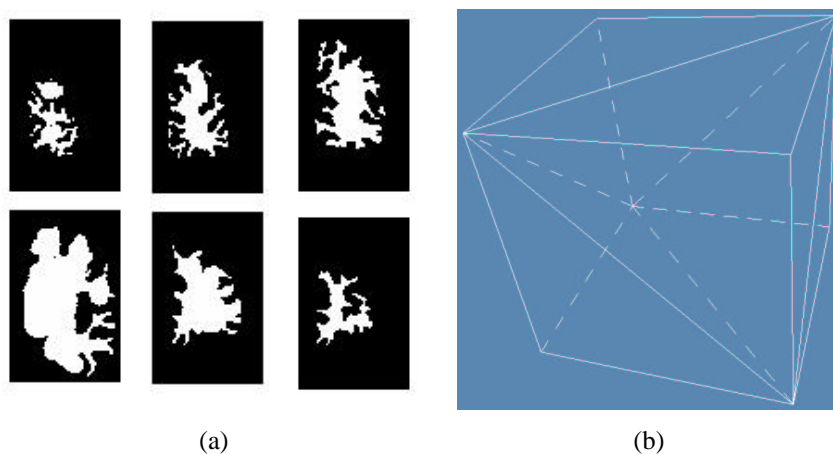
(a)   (b)

FIG. 2. *(a) are some binary brain images, where white pixels are inside brain and black pixels are outside brain. (b) is a cube consisted of 5 tetrahedra. Our volume tetrhedralization method read in binary images and output tetrahedral structure in the space.*

The algorithm is given below.

ALGORITHM 2. *Sphere Carving Algorithm*
Input (a sequence of volume images and a desired surface genus number),
Output (a tetrahedral mesh whose surface has the desired genus number).

> 1. *Build a solid sphere tetrahedral mesh consisted of tetrahedra, such that the sphere totally enclose the 3D data. Let the boundary of the solid sphere be S;*
> 2. *Put all the tetrahedra which share faces with S in a queue Q, the elements in Q is sorted by the sharing face number, the first in the queue is the one which shares the most number of faces with S;*
> 3. *Exit if Q is empty, otherwise pop out the first tetrahedron, t, from Q;*
> 4. *If t is not inside the object and the new surface after removing it still has genus 0, then remove the tetrahedron from the mesh and go to Step 2; otherwise go to step 3.*

4. Experiments. In our experiments, we use tetrahedra to represent the volume data. We tested our algorithm on both synthetic and brain volume data. Our synthetic data is a cube consisting of many tetrahedra. Figure 3(a) shows the surface of a solid cube and (b) shows the cube in wireframe mode. We used the volumetric harmonic mapping algorithm to map it onto a solid sphere. Figure 3(c) shows the surface of a solid sphere onto which it harmonically mapped. Figure 3(d) shows the solid sphere in wireframe mode.

We also performed some experiments to study the harmonic map obtained. As shown in Figure 4, we assign a random color to each vertex of the cube model. We then removed some tetrahedra from the cube. We also remove these tetrahedra from the sphere. Since the cube has a convex surface, this shows that the mapping is a smooth bijection, i.e. diffeomorphism. Figure 5 shows another experiment. We started with a different surface condition (different conformal map on the surface via Möbius transformation). The harmonic map changes. We

embedded the bunny in the resulting using its barycentric coordinate. As expected, the bunny was severely distorted, showing that the adjusted boundary mapping is propagated to the interior as well.

To reduce memory requirements in the implementation, we use a multi-resolution method to represent the volume data. An example of surface genus zero volume is a brain volume. A coarse-scale brain model (which could be further refined) is shown in Figure 6(a) and (b). The volumetric brain harmonic mapping result is shown in Figure 6(c) and (d). We show this result at coarse scale to visualize the solution grid, but it can be further refined to capture greater geometric detail.

Figure 8 illustrates a volumetric harmonic map on a prostate model. A volumetric prostate model is built from a sequence of MRI images. As shown in Figure 7, the boundary of prostate in each image is hand-drawn by physicians in yellow line. With our sphere carving algorithm, we get volumetric prostate model 8(a) and (b). The harmonic map results are shown in Figure 8 (c) and (d).
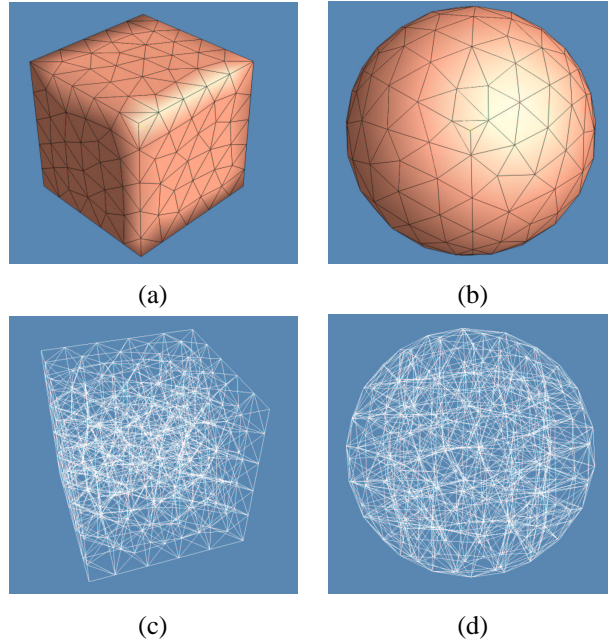

(a)   (b)

(c)   (d)

FIG. 3. *(a) and (b) are the volumetric data surface of a cube and its harmornic mapping to a sphere; (c) and (d) are the volumetric data represented in wireframe mode and its harmonic mapping to a sphere.*

5. Conclusion and Future Work. This paper introduces a volumetric harmonic map method. First we map the volumetric boundary conformally onto a sphere. Then with this boundary condition, we compute its harmonic map in the object interior with a heat flow method. Our work is general enough to be easily generalized to higher dimensional cases, or to other organ systems than brain, e.g. for representing cardiac motion. To apply this algorithm on brain mapping problem, we developed a novel algorithm to calculate the simplicial
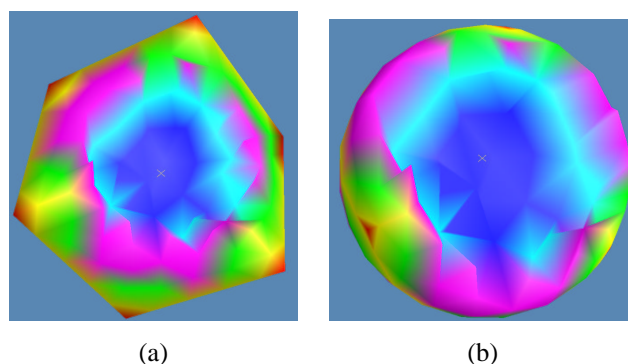
(a)   (b)

FIG. 4. *Illustrates the internal geometry after we removed the same tetrahedra from the solid sphere. This illustrates how the bijection maps simply connected regions to simply connected regions of the sphere, and points in the two coordinate systems can be associated.*

decomposition of volume adapted to surface. Our experimental results on both synthetic and brain MRI image data are promising.

Since the exterior brain surface is highly convoluted, computation of 3D harmonic maps is difficult. In the future, we will study the necessary and sufficient conditions for a 3D harmonic map to be diffeomorphic. We will also use non-structured tetrahedral mesh to represent brain volumetric data and test our algorithm on it.

REFERENCES

[1] D. ZHANG AND M. HEBERT, Harmonic maps and their applications in surface matching. In:IEEE Proceedings of Computer Vision and Pattern Recognition, volume 2, pages 524–530, 1999.

[2] X. GU, Y. WANG, T. CHAN, P. M. THOMPSON, AND S.-T. YAU, *Genus zero surface conformal mapping and its application to brain surface mapping*, In: Information Processing in Medical Imaging, pages 172–184, Ambleside, UK, July 2003.

[3] Y. WANG, X. GU, T. CHAN, P. M. THOMPSON, AND S.-T. YAU, *Intrinsic brain surface conformal mapping using a variational method*, In: SPIE International Symposium on Medical Imaging, 2004.

[4] J. C. GEE, *On matching brain volumes*, Pattern Recognition, 32(1999), pp. 99–111.

[5] M. FERRANT, S.K. WARFIELD, A. NABAVI, F.A. JOLESZ, AND R. KIKINIS, *Registration of 3d intraoperative MR images of the brain using a finite element biomechanical model*, In: MICCAI, pages 19–28, 2000.

[6] W. E. LORENSEN AND H. E. CLINE, *Marching cubes: A high resolution 3d surface construction algorithm*, In: Proceedings of SIGGRAPH 1987, pages 163–169, 1987.

[7] Y. ZHANG, C. BAJAJ, AND B.-S. SOHN, *Adaptive and quality 3d meshing from imaging data*, In: Proceedings of 8th ACM Symposium on Solid Modeling and Applications, pages 286–291, Seattle, WA, June 2003.
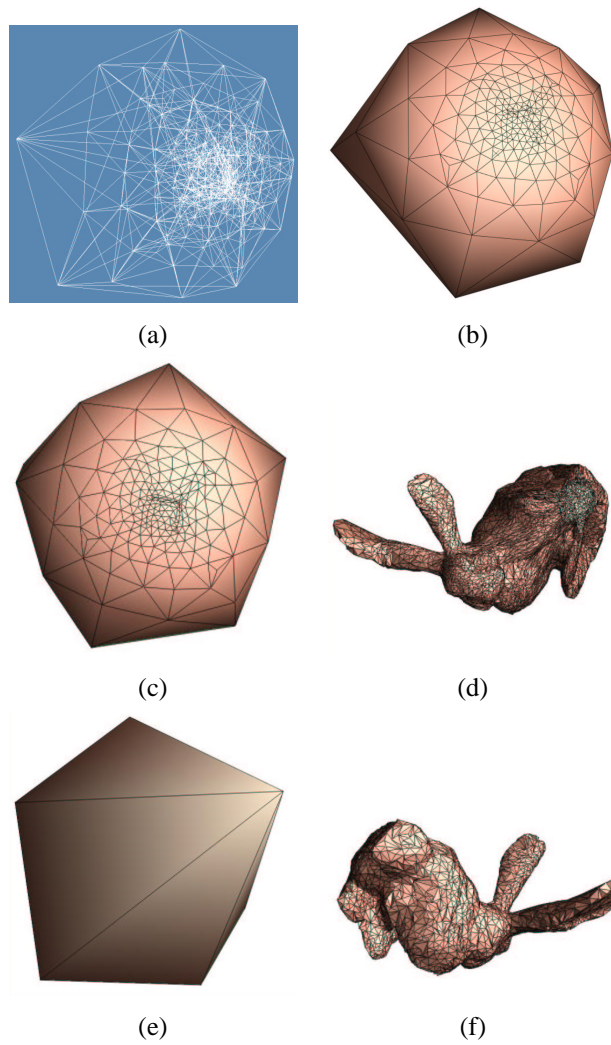
(a)

(b)

(c)

(d)

(e)

(f)

FIG. 5. *Illustrates the internal volume change when the surface mapping of a cube changes following a möbius transformation. (a) and (b) are volumetric view and surface view of a cube volumetric image in a sphere. A bunny is barycentric embedded into the sphere. (c),(d),(e),and (f) show some snapshots when we rotate the sphere. We can find the distortion on the bunny model which is due to the möbius transformation of the cube image on the sphere.*
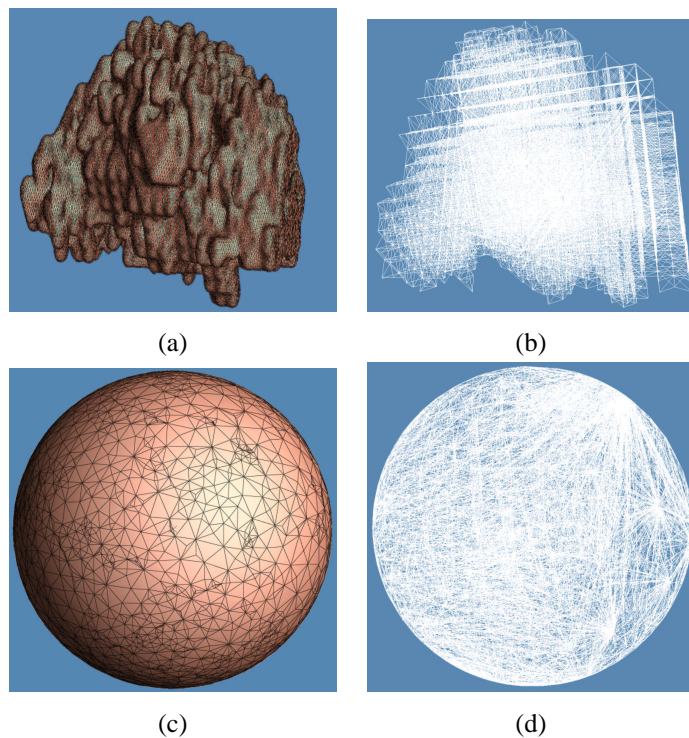
FIG. 6. *Illustrates volumetric brain harmonic mapping. (a) is the volumetric brain surface; (b) is the brain volume in wireframe mode; (c) is the surface of the brain volumetric harmonic map into a sphere; (d) is brain volumetric harmonic map into a sphere in wireframe mode.*
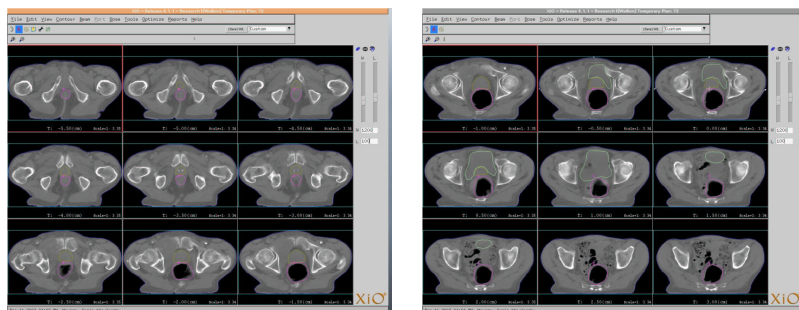

FIG. 7. *Illustrates the images data used to build volumetric prostate model. They are a sequence of MRI images. The prostate boundaries (yellow line) are hand-drawn by physicians.*
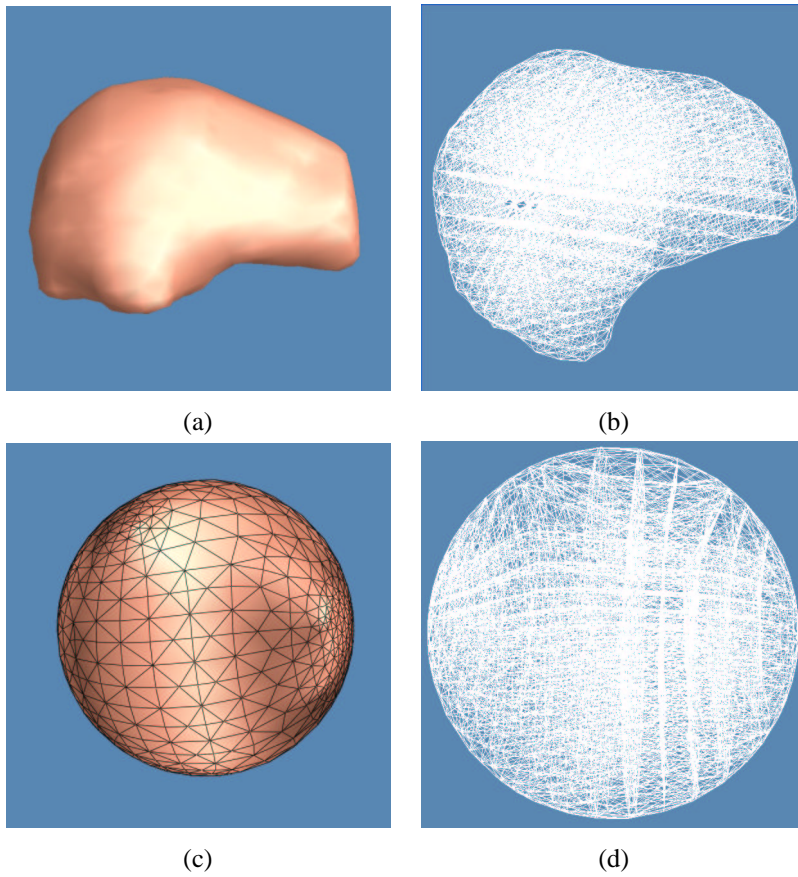
(a)

(b)

(c)

(d)

FIG. 8. *Illustrates volumetric prostate harmonic mapping. (a) is the volumetric prostate surface; (b) is the prostate volume in wireframe mode; (c) is the surface of the prostate volumetric harmonic map into a sphere; (d) is prostate volumetric harmonic map into a sphere in wireframe mode.*